

See discussions, stats, and author profiles for this publication at: <https://www.researchgate.net/publication/318985706>

Serum Iron Protects from Renal Postischemic Injury

Article in *Journal of the American Society of Nephrology* · August 2017

DOI: 10.1681/ASN.2016080926

CITATIONS

2

READS

52

25 authors, including:



Mariane Tami Amano
Hospital Sirio Libanes

56 PUBLICATIONS 307 CITATIONS

[SEE PROFILE](#)



Jonathan M Chemouny
French National Institute for Agricultural Research

30 PUBLICATIONS 126 CITATIONS

[SEE PROFILE](#)



Michael Dussiot
Paris Descartes, CPSC

75 PUBLICATIONS 1,148 CITATIONS

[SEE PROFILE](#)



Sanae Ben Mkaddem
French Institute of Health and Medical Research

54 PUBLICATIONS 879 CITATIONS

[SEE PROFILE](#)

Some of the authors of this publication are also working on these related projects:



Renal transplattation [View project](#)



Deciphering pathophysiological crosstalk of glomerular cells [View project](#)

Serum Iron Protects from Renal Postischemic Injury

Céline Vaugier,^{*†‡§} Mariane T. Amano,^{||} Jonathan M. Chemouny,^{¶**††‡‡} Michael Dussiot,^{*†‡§} Claire Berrou,^{*†‡§} Marie Matignon,^{§§} Sanae Ben Mkaddem,^{¶**††} Pamela H.M. Wang,^{*†‡§} Aurélie Fricot,^{*†‡§} Thiago T. Maciel,^{*†‡§} Damien Grapton,^{*†‡§} Jacques R.R. Mathieu,^{||||} Carole Beaumont,^{¶¶} Marie-Noëlle Peraldi,^{***} Carole Peyssonnaud,^{||||} Laurent Mesnard,^{††††‡‡§§§§} Eric Daugas,^{¶**††‡‡} François Vrtovsnik,^{¶**††‡‡} Renato C. Monteiro,^{¶**††||||} Olivier Hermine,^{*†‡§¶¶¶¶} Yelena Z. Ginzburg,^{††††} Marc Benhamou,^{¶**††} Niels O.S. Camara,^{||} Martin Flamant,^{¶**††‡‡‡‡} and Ivan C. Moura^{*†‡§****}

*Institut National de la Santé et de la Recherche Médicale Unité Mixte de Recherche (UMR)1163, Paris, France; †Sorbonne Paris Cité, Université René Descartes, Imagine Institute, Paris, France; ‡Centre National de la Recherche Scientifique Equipe de Recherche Labellisée (ERL)8254, Paris, France; §Laboratoire d'excellence GR-Ex, Paris, France; ||Laboratory of Transplantation Immunobiology, Department of Immunology, Institute of Biomedical Sciences IV, University of São Paulo, Sao Paulo, Brazil; ¶Université Denis-Diderot, Laboratoire d'excellence INFLAMEX, Paris, France; **UMR1149, Paris, France; ††ERL8252, Paris, France; ‡‡Departments of Nephrology, ||||Immunology, and ††††Physiology, Assistance Publique-Hôpitaux de Paris (AP-HP), Hôpital Bichat-Claude Bernard, Paris, France; §§Department of Nephrology and Transplantation, AP-HP, Hôpital Henri Mondor, Institut Francilien de recherche en Néphrologie et Transplantation, Paris-Est Université, Creteil, France; ||||UMR1016, Paris, France; ¶¶UMR773, Paris, France; ***UMR 940, Paris, France; †††UMR702, Paris, France; ‡‡‡Urgences Néphrologiques et Transplantation Rénale, AP-HP, Hôpital Tenon, Paris, France; §§§Université Pierre et Marie Curie, Paris, France; ¶¶¶Department of Clinical Hematology, AP-HP, Hôpital Necker-Enfants Malades, Paris, France; ****Equipe labellisée LIGUE 2015, Paris, France; and ††††Erythropoiesis Laboratory, Lindsey F. Kimball Research Institute, New York Blood Center, New York, New York

ABSTRACT

Renal transplants remain a medical challenge, because the parameters governing allograft outcome are incompletely identified. Here, we investigated the role of serum iron in the sterile inflammation that follows kidney ischemia-reperfusion injury. In a retrospective cohort study of renal allograft recipients ($n=169$), increased baseline levels of serum ferritin reliably predicted a positive outcome for allografts, particularly in elderly patients. In mice, systemic iron overload protected against renal ischemia-reperfusion injury-associated sterile inflammation. Furthermore, chronic iron injection in mice prevented macrophage recruitment after inflammatory stimuli. Macrophages cultured in high-iron conditions had reduced responses to Toll-like receptor-2, -3, and -4 agonists, which associated with decreased reactive oxygen species production, increased nuclear localization of the NRF2 transcription factor, increased expression of the NRF2-related antioxidant response genes, and limited NF- κ B and proinflammatory signaling. In macrophage-depleted animals, the infusion of macrophages cultured in high-iron conditions did not reconstitute AKI after ischemia-reperfusion, whereas macrophages cultured in physiologic iron conditions did. These findings identify serum iron as a critical protective factor in renal allograft outcome. Increasing serum iron levels in patients may thus improve prognosis of renal transplants.

J Am Soc Nephrol 28: ●●–●●●, 2017. doi: <https://doi.org/10.1681/ASN.2016080926>

Received August 31, 2016. Accepted June 30, 2017.

Published online ahead of print. Publication date available at www.jasn.org.

Correspondence: Dr. Ivan C. Moura, Institut National de la Santé et de la Recherche Médicale–Unité Mixte de Recherche 1163, Institut Imagine, 24 Bd du Montparnasse, 75015 Paris, France. Email: ivan.moura@inserm.fr

Copyright © 2017 by the American Society of Nephrology

Although it is not the only one, organ transplantation may be the best option for many patients faced with end stage renal failure. The biologic parameters that determine graft outcome are many, and most relate to the immune system, such as the histocompatibility determinants expressed on graft and host cells. In any case, when the graft is rejected, this is implemented by the host immune and inflammatory cells. Despite considerable progress in the understanding of graft rejection mechanisms, long-term graft survival remains a challenge. Delayed graft function affecting both short- and long-term graft survival^{1–3} is a consequence of ischemia-reperfusion injury (IRI),⁴ an inflammatory reaction that occurs in allografts after transplantation, despite various preventive strategies.⁵ Interestingly, a growing body of evidence suggests that iron homeostasis plays a critical role in the modulation of inflammatory responses. Monocytes from patients on dialysis with high serum ferritin (*i.e.*, increased serum iron load) showed decreased production of proinflammatory cytokines.⁶ High-iron culture conditions of the THP-1 monocytic cell line and PBMCs resulted in decreased IFN- γ responses to cell stimulation.^{7,8} In *Hfe* knockout (*Hfe*^{-/-}) mice, a constitutive iron overload model, decreased inflammatory responses were observed.⁹ Conversely, exacerbated inflammatory responses were reported in experimental mouse models of iron deficiency. Mice with iron-deficient diet or iron-refractory iron deficiency had increased susceptibility to endotoxic shock, and their macrophages showed increased IL-6 and TNF- α mRNA levels after LPS challenge.¹⁰ Altogether, these results suggest an anti-inflammatory role for iron through a still unknown molecular mechanism.¹¹ Yet, these data contradict a large body of literature suggesting a proinflammatory role of excess iron through its participation in the Fenton reaction, the production of reactive oxygen species (ROS), and the activation of NF- κ B pathways.^{12–16} Thus, the effect of iron on the IRI affecting grafted organs, which determines the long-term success of transplantation, remains unresolved. Here, we addressed this question in a model of sterile renal inflammation and cohorts of patients with kidney transplants. Our data identify serum iron as a strong protective factor.

RESULTS

High Ferritin Level Is a Good Prognostic Marker in Kidney Transplantation

Management of anemia in patients with ESRD frequently involves erythropoietin and intravenous iron administration. Yet, the contribution of iron load to renal allograft outcome is incompletely understood. We performed a retrospective cohort study and stratified a population of renal allograft recipients ($n=169$) according to baseline serum ferritin concentration, a reliable marker of systemic iron status. Patients exhibiting serum ferritin >600 ng/ml (high-ferritin first quartile group; $n=42$) were compared with patients exhibiting low ferritin (<600 ng/ml; $n=127$) (Table 1). Serum iron and transferrin saturation (TSAT) were increased, and total iron binding capacity (TIBC) was reduced in patients with high ferritin,

whereas C-reactive protein levels were comparable, confirming increased systemic iron status in the high-ferritin group (Supplemental Figure 1, A–D). Hemoglobin levels were comparable between the two groups (Supplemental Figure 1E). Within the >50 -year-old patient group and relative to patients with low ferritin, patients with high ferritin exhibited improved kidney function 7 days post-transplantation as measured by eGFR using the abbreviated Modification of Diet in Renal Disease equation (eGFR_{MDRD}) (Figure 1A). There was no statistical difference when the whole population was analyzed or when only patients <50 years old were taken into account. We believe that this is due to increased risk of vascular lesions and increased susceptibility to IRI lesion with age. Other factors that could influence allograft function (living versus deceased donor, cause of ESRD, dual kidney transplantation, episodes of early acute rejection, donor age, donation after acute kidney failure, and cold ischemia time) were not significantly different between high- and low-ferritin groups (Table 1).

In the entire cohort, 42 patients of those with available GFR measurement 1 year post-transplantation were over 50 years old. In this group, serum ferritin correlated with measured GFR (mGFR) (Figure 1B), further suggesting that evaluation of serum ferritin could help to predict long-term allograft function in these patients. Of note, serum ferritin in the high-ferritin group exceeded all international standard recommendations for patients with ESRD.^{17,18} Moreover, analysis of graft survival up to 8 years in the cohort of patients confirmed that >50 -year-old patients with high ferritin levels at the time of transplantation have increased graft survival (Figure 1, C and D). Death-censored graft survival did not reach significance in the >50 -year-old patients with high ferritin, most probably because of the lower number of events (Supplemental Figure 1, F and G).

Iron Protects the Kidney from Ischemic Injury

To gain further mechanistic insights, we subjected *Hfe*^{-/-} mice to ischemic kidney injury to mimic ischemia occurring during kidney transplantation.¹⁹ These mice present progressive iron overload with high serum iron and increased TSAT at 12 weeks of age²⁰ (Table 2) without significant changes in red blood cells, circulating leukocytes, and lymphocytes. In addition, we also observed an increased mean corpuscular hemoglobin in *Hfe*^{-/-} mice (Table 2).

Wild-type (WT) and *Hfe*^{-/-} mice were subjected to bilateral 45-minute renal pedicle clamping or sham operated followed by 24 hours of reperfusion. Acute tubular necrosis lesions, including tubular epithelial cell damage and dilated tubules with casts, observed in WT mice were dramatically reduced in *Hfe*^{-/-} mice (Figure 1E, Supplemental Figure 2A). Accordingly, reduced serum creatinine and BUN levels were observed in *Hfe*^{-/-} relative to WT mice after postischemic reperfusion (Figures 1, F and G). This protective effect persisted 48 hours after reperfusion (not shown).

IRI is a well known model to study sterile inflammation,²¹ in which neutrophils and macrophages are key players promoting acute tissue injury.¹⁹ As expected and compared with controls, recruitment of GR1⁺ and CD11b⁺ inflammatory cells was greatly increased in WT mice after IRI, concurrent with increased

Table 1. Baseline characteristics of kidney allograft recipients according to ferritin levels before transplantation

Parameter	Total	Low Ferritin	High Ferritin	P Value
No.	169	127	42	
Ferritin, ng/ml		10–594	608–1925	
Recipient characteristics				
Men, % (no.)	61.5 (104)	65.4 (83)	50.0 (21)	0.10
Age, yr	49.6±13.0	48.4±13.2	53.1±11.9	0.04
Dialysis mode, % (no.)				<0.01
Hemodialysis	83 (140)	77 (98)	100 (42)	
Peritoneal	5 (8)	6 (8)	0	
Preemptive	9 (16)	13 (16)	0	
Unknown	3 (5)	4 (5)	0	
Cause of ESRD, % (no.)				0.65
Diabetes mellitus	21 (36)	21 (27)	21 (9)	
Glomerular disease	17 (28)	18 (23)	12 (5)	
Hypertension	15 (26)	15 (19)	17 (7)	
PKD	12 (20)	11 (14)	14 (6)	
Congenital uropathy or reflux	3 (5)	4 (5)	0 (0)	
Other known diagnoses	13 (22)	12 (15)	17 (7)	
Unknown	19 (32)	19 (24)	19 (8)	
Donor characteristics				
Age, yr	50.0±14.5	49.2±14.5	52.3±14.3	0.25
Type of donation, % (no.)				0.60
Living	14 (23)	13 (16)	17 (7)	
Cadaveric	86 (146)	87 (111)	83 (35)	
Transplantation characteristics				
Transplanted organ, % (no.)				0.76
Kidney	91 (154)	91 (115)	93 (39)	
Combined kidney-pancreas	9 (15)	9 (12)	7 (3)	
Cold ischemia time, h	13.7±6.8	13.6±6.4	14.2±8.1	0.58
Acute rejection during first year post-transplantation, % (no.)				0.69
Yes	5 (9)	5 (6)	7 (3)	
No	95 (160)	95 (121)	93 (39)	

To convert to SI unit, multiply ferritin by one to obtain micrograms per liter. Statistical analyses performed were Fisher exact test for sex, type of transplantation, donor type, and acute rejection; chi-squared test for dialysis mode and cause of ESRD; and unpaired *t* test for recipient age at transplantation, donor age, and cold ischemia time. Categorical data are expressed as percentages (numbers), and recipient age at transplantation, donor age, and cold ischemia time are expressed as means±SEM. PKD, polycystic kidney disease.

proinflammatory cytokines. In contrast, *Hfe*^{-/-} mice presented minimal recruitment of inflammatory cells and basal IL-6, MCP-1, and TNF- α responses (Figure 1, H and I, Supplemental Figure 2, B and C). Mobilization of circulating inflammatory cells was greatly reduced in *Hfe*^{-/-} versus WT mice, suggesting that reduced inflammatory response in *Hfe*^{-/-} mice was a consequence of reduced myeloid cell mobilization from bone marrow (Supplemental Figure 2, D and E).

In bone marrow reconstitution experiments, WT animals adoptively transferred with *Hfe*^{-/-} bone marrow cells were only minimally protected against IRI (Figure 1J), whereas *Hfe*^{-/-} mice reconstituted with WT myeloid cells remained completely protected against IRI (Figure 1K). This showed that HFE deficiency in myeloid cells²² is not the main protective factor against IRI in HFE-deficient animals but rather, suggested the involvement of iron overload in these animals.

Iron Prevents Mobilization of Inflammatory Macrophages

To examine the effect of iron on inflammatory responses, we injected WT mice with iron sucrose solution (Venofer). Both

Venofer- and vehicle-treated mice were then injected intraperitoneally with LPS, and myeloid inflammatory cells in the peritoneum were counted.²³ Elicitation of peritoneal inflammatory macrophages by LPS has been reported to be due to recruitment of blood monocytes and not to their generation from resident peritoneal macrophages.²³ LPS induced no change in resident macrophage numbers (large peritoneal macrophages, CD11b^{high}F4/80^{high}Ly6G⁻Ly6C⁺ cells) but did induce an increase in neutrophil (CD11b⁺GR1⁺ cells) numbers that was identical in Venofer- and PBS-treated mice. As expected, LPS induced an increased number of inflammatory macrophages (small peritoneal macrophages, CD11b^{low}F4/80^{low}Ly6G⁻Ly6C⁻ cells) in PBS-treated mice. This increase was drastically prevented in Venofer-treated mice (Figure 2A, Supplemental Figure 3A).

Iron Dampens Macrophage Responsiveness to Inflammatory Stimuli

To study the effect of systemic iron load on macrophage phenotype, bone marrow-derived macrophages (BMMs) were differentiated in the absence or presence of soluble iron

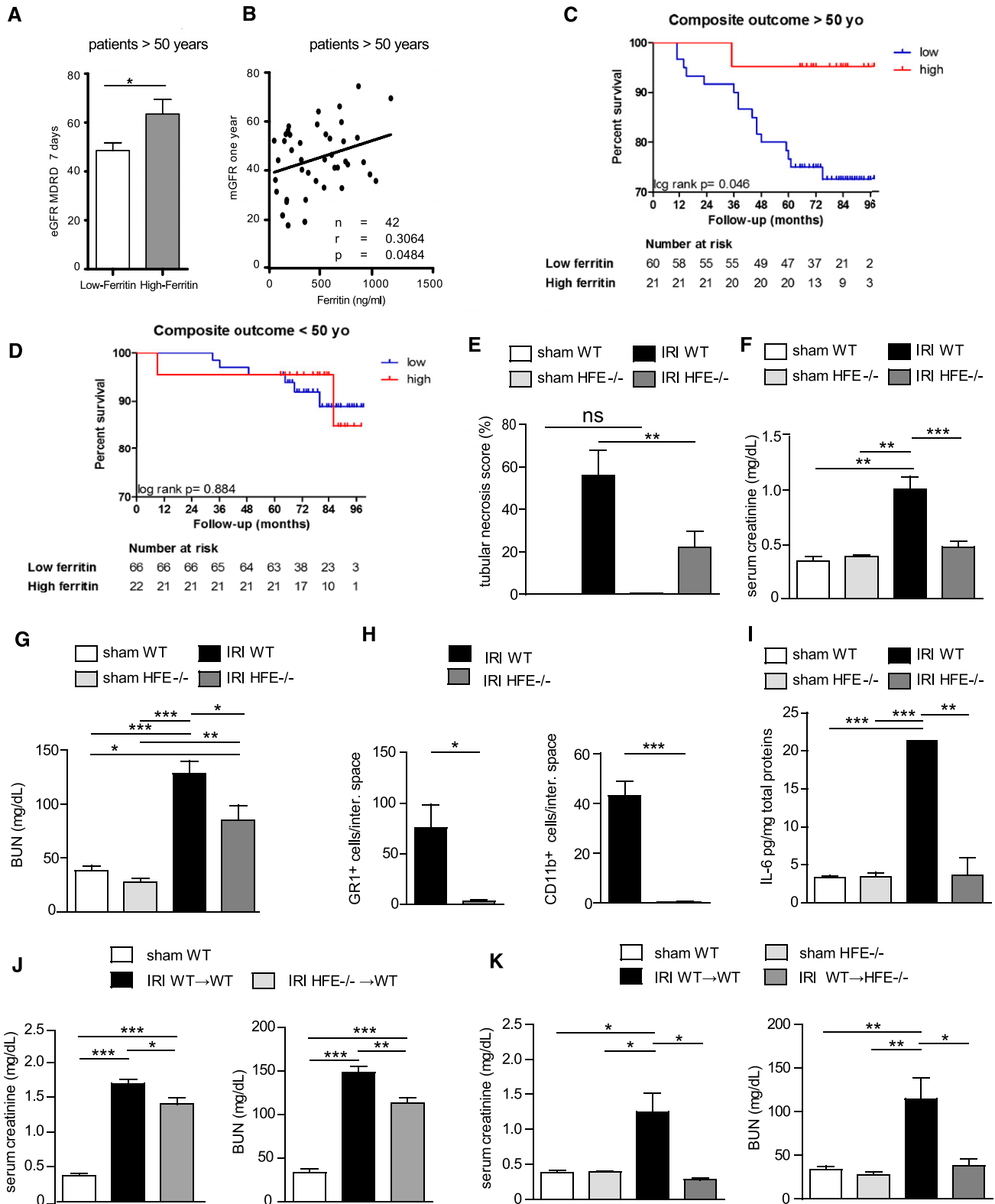


Figure 1. High serum iron is protective in IRI. (A–D) Increased serum ferritin levels are associated with improved outcome of kidney allografts. High ferritin: patients in the fourth quartile (>600 ng/ml). Low ferritin: patients in the first to third quartiles (<600 ng/ml). (A) eGFR_{MDRD} at day 7 from renal transplantation in elderly patients (n=147). (B) Correlation of mGFR 1 year after renal transplantation with baseline serum ferritin levels in >50-year-old patients (n=42). (C and D) Kidney transplant survival (composite outcome: death or graft loss) up to 8 years in (C) >50-year-old patients and (D) <50-year-old patients. (E–K) Iron overload protects against IRI in mice. WT or

(Fe-nitritolriacetate) at two concentrations (20 and 60 μM). Neither cell morphology nor expression of cell surface markers (CD11b and F4/80) were altered by iron (Supplemental Figure 3, B and C), suggesting that macrophage differentiation was unaffected. However, macrophages differentiated in the presence of iron were unable to upregulate CD86 in response to TLR4 (LPS), TLR3 (poly I:C), and TLR2 (peptidoglycan) agonists (Figure 2B, Supplemental Figure 3D). Iron-induced macrophage unresponsiveness to LPS was observed whether LPS was added on day 0 or when cells were almost completely differentiated (90% CD11b⁺ F4/80⁺ BMM) on day 4 (Supplemental Figure 3E).

Venn diagram analysis of Affymetrix microarray chips of macrophages differentiated in the presence or absence of soluble iron and stimulated or not stimulated with LPS confirmed that the overall response to LPS differed between control macrophages (BMMs) and iron-treated bone marrow-derived macrophages (Fe-BMMs) (Supplemental Figure 4A). Genes implicated in inflammatory response were downregulated after LPS treatment in Fe-BMM compared with BMM (Supplemental Figure 4, B and C) as well as genes involved in NF- κ B responses (not shown). Consistent with these findings, LPS Fe-BMM showed impaired secretion of TNF- α , MCP-1, and IL-6 (Supplemental Figure 4D).²⁴

Iron Activates Antioxidant Response through NRF2 in Macrophages

Increased expression of antioxidant genes (Figure 2C) and impaired ROS production on LPS treatment (Figure 2D, Supplemental Figure 5A) were observed in Fe-BMM compared with BMM. Therefore, iron induced antioxidant gene expression, prevented ROS response to inflammatory stimuli, decreased proinflammatory cytokine secretion and expression of activation markers, and impaired activation of the NF- κ B pathway in primary macrophages.

One of the transcription factors that control antioxidant response gene expression is NRF2.^{25–27} Under normal conditions, NRF2 is rapidly degraded in the cytoplasm.²⁸ During oxidative stress, NRF2 translocates into the nucleus, where it binds to the promoter region of antioxidant response genes, initiating their transcription.²⁹ Iron alone induced the recruitment of NRF2 into BMM nuclei (Figure 2E), indicating that NRF2 activation is an iron-responsive transcription factor. In addition, iron-induced inhibition of BMM activation by LPS was significantly impaired in *Nrf2*^{-/-} BMM (Supplemental Figure 5, B and C). Finally, iron treatment did not induce M1 or M2 polarization but decreased PS exposure, suggesting an increased survival of these cells (Figure 2, F and G).

Table 2. Baseline serum iron parameters and full blood count in WT and *Hfe*^{-/-} mice

Parameter	HFE ^{+/+}	HFE ^{-/-}	P Value
RBC, 10 ⁶ / μl	8.67 \pm 0.32	8.84 \pm 0.21	0.20
MCV, fl	55.6 \pm 1.46	58.4 \pm 0.77	0.06
Hematocrit, %	48.1 \pm 1.51	51.6 \pm 0.88	0.07
MCH, pg	17.9 \pm 0.23	18.5 \pm 0.1	0.04
MCHC, g/dl	32.4 \pm 0.67	31.7 \pm 0.55	0.70
Hemoglobin, g/dl	15.5 \pm 0.49	16.4 \pm 0.44	0.12
RDW-SD, %	29.9 \pm 0.34	30.1 \pm 0.09	0.80
RDW-CV, %	14.7 \pm 0.39	13.9 \pm 0.22	0.09
Platelets, 10 ³ / μl	349.6 \pm 60.2	402.8 \pm 45.6	0.80
Lymphocytes, 10 ³ /mm ³	5.2 \pm 0.75	3.45 \pm 0.51	0.14
Monocytes, 10 ³ /mm ³	0.49 \pm 0.2	0.22 \pm 0.08	0.47
Neutrophils, 10 ³ /mm ³	1.5 \pm 0.56	0.67 \pm 0.25	0.43
Iron, $\mu\text{mol/L}$	12.9 \pm 4.39	61.5 \pm 1.38	0.03
Transferrin, g/L	1.73 \pm 0.07	1.53 \pm 0.10	0.16
Ferritin, ng/L	274.9 \pm 42.6	245.4 \pm 49.9	0.48
TSAT, %	30.4 \pm 10.6	161.3 \pm 6.94	0.03

RBC, red blood cell; MCV, mean cell volume; MCH, mean corpuscular hemoglobin; MCHC, mean corpuscular hemoglobin concentration; RDW-SD, red blood cell distribution width-standard deviation; RDW-CV, red blood cell distribution width-coefficient of variation.

Iron Prevents Macrophage-Dependent Kidney Ischemic Injury

Macrophage depletion by clodronate liposomes abrogates IRI in mice. We reconstituted clodronate liposome-treated animals with macrophages that were derived in the presence of physiologic and supraphysiologic iron conditions (Figure 3A). Macrophages differentiated in the presence of supraphysiologic iron conditions could not reconstitute kidney injury conversely to those differentiated in physiologic iron conditions (Figure 3, B and C), in spite of an apparently unchanged histology (Figure 3D) (data not shown).

DISCUSSION

In this study, we identified serum iron as a critical modulator of IRI, an inflammatory insult that damages transplanted organs. We show that increased serum iron is associated with improved graft function, with serum ferritin having a high predictive value, and that protection by iron is due to the down-modulation of macrophage responsiveness to inflammatory stimuli after upregulation of NRF2-dependent antioxidant response gene expression.

The fact that serum iron is protective in organ transplantation is strongly supported by our observation that, in patients with

Hfe^{-/-} mice were subjected to bilateral ischemia or sham operated and euthanized 24 hours after reperfusion. (E) Tubular necrosis score in cortical medullary junction areas ($n=5-11$ mice per group). Ten fields per kidney were evaluated as well as (F) serum creatinine, (G) BUN levels ($n=5-19$), (H) GR1⁺ and CD11b⁺ cells in interstitial (inter.) space (ten fields per mouse; $n=4$ mice per group), and (I) IL-6 in kidney extracts ($n=4$ mice per group). (J and K) Indicated irradiated mice were reconstituted (\rightarrow) with the indicated bone marrow cells. Eight weeks later, mice were subjected to IRI or sham operated. BUN and serum creatinine were assessed 24 hours later ($n=4-9$ mice per group). Mean \pm SEM of three to five experiments. * $P<0.05$; ** $P<0.01$; *** $P<0.001$.

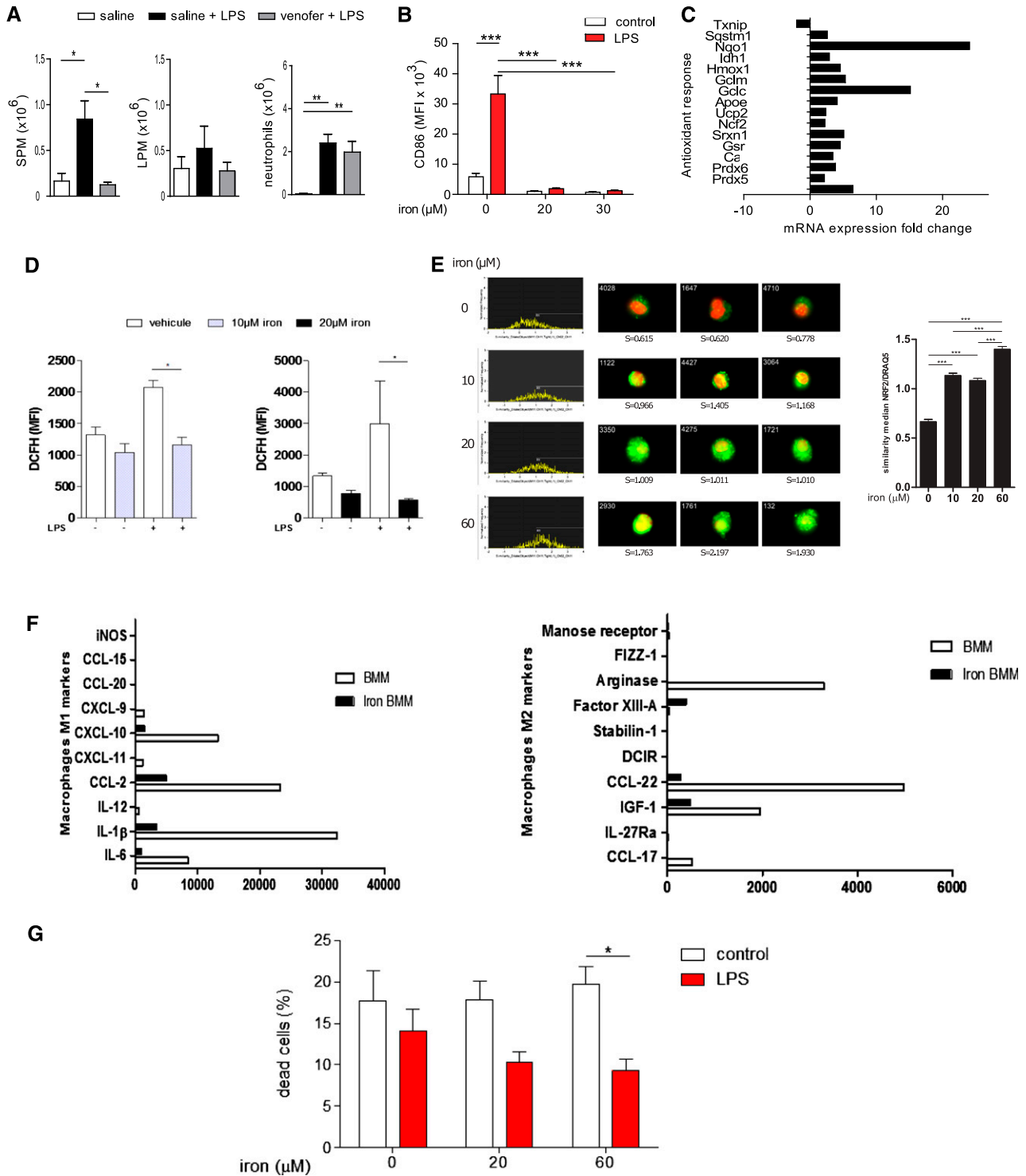


Figure 2. Iron blocks macrophage inflammatory response through antioxidant gene transcription on NRF2 mobilization. (A) Impaired inflammatory macrophage recruitment. Mice were injected intraperitoneally for 10 days with saline or iron sucrose solution (Venofen) before LPS challenge. Absolute numbers of small peritoneal macrophages (SPMs), large peritoneal macrophages (LPMs), and neutrophils (CD11b⁺Ly6G⁺) in the peritoneal cavity were counted ($n=4$ mice per group). (B) Impaired macrophage inflammatory responses. BMMs were differentiated in the absence or presence of iron. At day 7 of culture, cells were stimulated overnight with LPS. Macrophage activation was evaluated by CD86 expression. One representative of four experiments. (C) Fold change variations of antioxidant response genes in macrophages cultured in the presence or absence of iron. (D) ROS production by macrophages cultured in the presence of iron and stimulated with LPS. ROS were measured by dichloro-dihydro-fluorescein diacetate (DCFH) fluorescence analyzed

kidney transplants, serum ferritin levels reliably predicted a positive outcome of renal allografts. In a recent paper, Eisenga *et al.*³⁰ draw conclusions that are in agreement with our study (*i.e.*, that iron deficiency is associated with a higher risk of mortality in patients with renal transplants that is independent of anemia). Our observation may be extended to other organ transplantation, because the genetic footprint of genes involved in iron metabolism and hepcidin and ferritin serum levels distinguished tolerant from nontolerant liver transplant recipients after withdrawal of immunosuppressive drugs.¹¹ These observations make serum iron attractive as an effective prognosis factor in organ transplantation, at least in over 50-year-old patients. In these patients, IRI is more prevalent and may be responsible for poorer prognosis of graft survival. In these patients, documenting the serum iron status of recipients before transplantation could help to intervene beforehand for an improved long-term graft survival. This could be done before surgery by intravenous administration of iron. Of note, this is currently performed to treat anemia, showing that serum iron can be pharmacologically modulated and thus, providing an easy therapeutic intervention tool. Although iron overload is associated with several complications, such as enhanced susceptibility for infections, we found no difference in BK virus infection between high- and low-ferritin groups (10% versus 15%, respectively, in the high quartile; chi-squared test; $P=0.40$).

However, great care should be taken before implementing such an option. Indeed, despite a number of studies documenting the ability of iron to reduce or prevent inflammatory responses both *in vitro* and *in vivo* (*e.g.*, our data), a major drawback for a transfer to the clinic is in the many reports showing the participation of excess iron in the Fenton reaction, the production of ROS, and the activation of NF- κ B pathways.^{12–16} We speculate that different inflammatory processes may be affected by iron in different ways. Indeed, we previously reported that iron modulates myelopoiesis, favoring neutrophil over monocyte lineage differentiation.³¹ Together with other reports,^{6–10} our observation that iron dampens macrophage inflammatory responses suggests that iron is an important down-modulator of the monocyte/macrophage lineage at both the differentiation and the activation levels. We propose that iron protects against diseases in which this lineage plays a pivotal role but that it could be deleterious when other cell types, such as neutrophils, are critically involved. This would explain why, in IRI, which is abrogated by macrophage depletion, iron is protective. The multifaceted actions of iron should, therefore, be

thoroughly documented, and careful studies in animal models should be initiated to test its effect on organ transplantation *per se* before any transfer to the clinic of intravenous administration of iron to prepare graft recipients.

The involvement of the transcription factor NRF2 identifies another pharmacologic target for therapeutic intervention. Indeed, NRF2 is shown here to be protective, because iron's action depended, at least in part, on NRF2. Of note, this action involved NRF2 translocation into the nucleus, where it could activate the transcription of antioxidant genes. This showed that increased expression of NRF2 is not the sole mode through which this transcription factor is regulated and that a more direct activation involving its intracellular redistribution is induced by iron. Interestingly, a recent report showed that NRF2 is also protective in crescentic GN.³² Pharmacologic activation of NRF2 or support of NRF2 activation may thus represent an alternative or complementary therapeutic approach in renal transplantation.

In summary, here we describe a role for serum iron load as an anti-inflammatory agent, which acts by preventing inflammatory macrophage responses in both animal models and patients with kidney transplants. Surprisingly, in humans, this association was relevant in over 50-year-old (but not in younger) patients, most probably because of their increased risk of vascular lesions and increased susceptibility to IRI lesion with age. These data support the 2016 Kidney Disease Improving Global Outcomes (KDIGO) guidelines for iron treatment and erythropoiesis-stimulating agent therapies in patients with CKD who are candidates for kidney transplantation.

CONCISE METHODS

Study Approval

All patients gave their informed consent for scientific use of anonymous data. All animals were treated in accordance with INSERM guidelines, and animal experiments adhered to the National Institutes of Health guide for the care and use of laboratory animals.

Patients

Patients from the Saint Louis hospital and Hôpital Bichat-Claude Bernard (AP-HP, Paris, France) who received kidney allografts from living or brain-dead donors between January 1, 2008 and October 20, 2011 were considered for this study. We included patients whose serum ferritin levels were assessed on the day of renal transplantation. Patients

by flow cytometry. (E) Cytoplasm to nucleus translocation of NRF2 analyzed by Imagestream multispectral imaging flow cytometer in WT BMMs differentiated in the absence or presence of iron. (Left panels) Similarity plots and three representative composite images of cells stained with DRAQ5 (red) and NRF2 (green). Nuclear translocation of NRF2 was measured using the similarity score (S). (Right panel) Quantification of similarity scores in all conditions (2000 images per condition). (F) Relative expression of M1 (left panel) and M2 (right panel) markers in BMMs treated or not treated with 20 μ M iron for 6 days as expressed as fold increase mRNA normalized to glyceraldehyde-3-phosphate dehydrogenase (GAPDH) and β -actin values in a combined way. (G) Percentage of annexin V–exposing BMMs treated or not treated with 20 and 60 μ M iron for 6 days and stimulated or not stimulated with LPS for 24 hours. Values are means \pm SEM of at least three experiments. MFI, mean fluorescence intensity. * $P<0.05$; ** $P<0.01$; *** $P<0.001$.

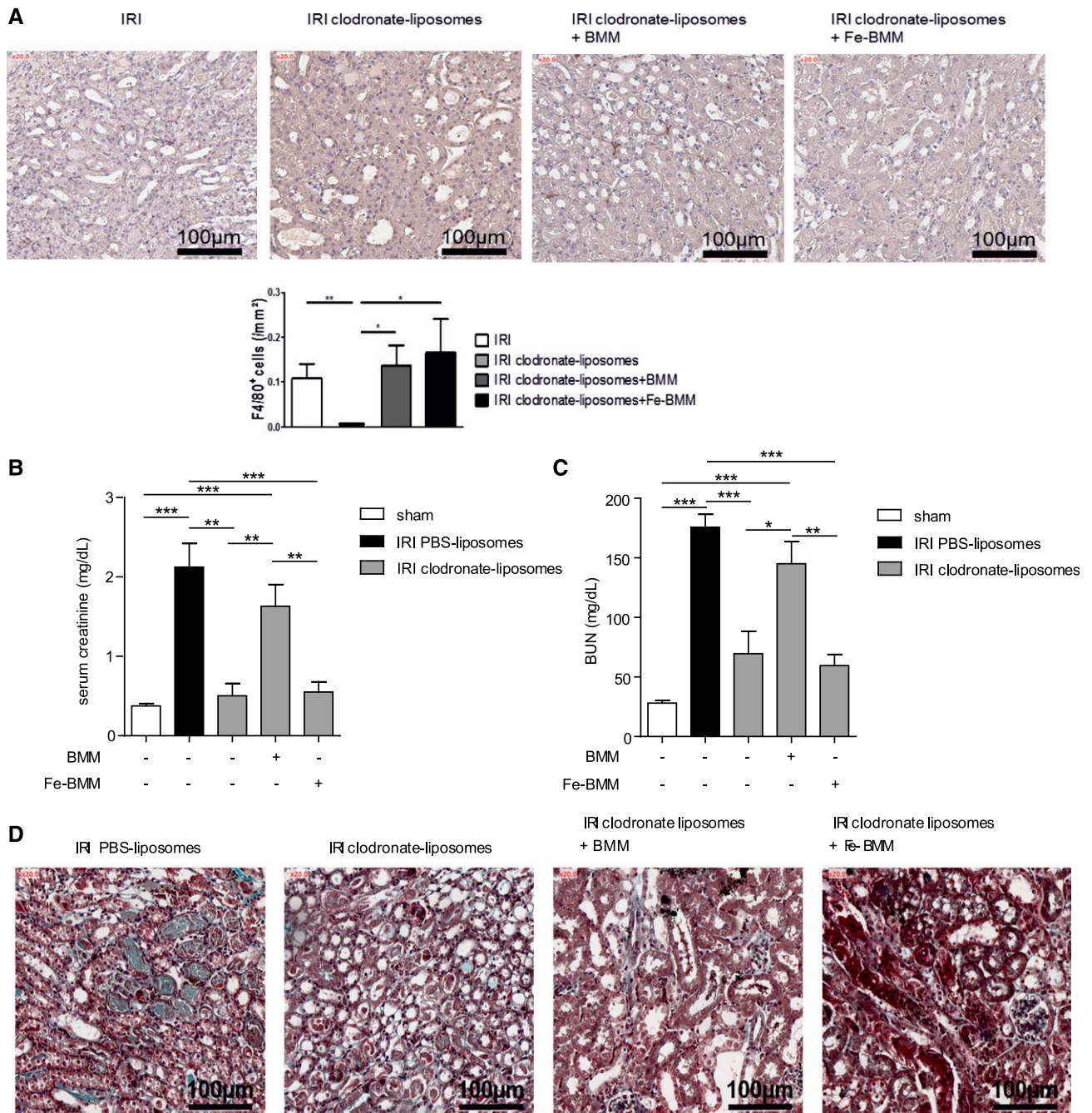


Figure 3. Macrophages differentiated in the presence of high iron levels are unable to support IRI. Mice were injected with 200 µl liposomes containing PBS or clodronate 48 hours before surgery. Animals were then subjected to 40 minutes of bilateral ischemia or sham operated. At 1 hour of reperfusion, BMMs differentiated in the presence of 60 µM iron (Fe-BMM) or control BMMs were administered by intravenous injection, and mice were euthanized at 24 hours of reperfusion. Blood samples were collected, and kidneys were removed for histologic analysis. (A) F4/80 labeling of tissue sections. Quantifications are shown. (B) Serum creatinine and (C) BUN levels in control and reconstituted mice (n=6–8 mice). Values are means±SEM. *P<0.05; **P<0.01; ***P<0.001. (D) Representative morphology (Masson trichrome staining) of the cortical-medullary junction from sham or IRI mice.

were divided into two groups according to their baseline serum ferritin levels being in the fourth quartile (high-ferritin group) or the first, second, and third quartiles (low-ferritin group). The hemoglobin values before transplantation were not found to be different according to the

quartile of ferritinemia (12.58±1.41, 11.87±1.70, 11.9±1.35, and 12.34±1.9 for quartiles 1–4, respectively; P=0.35; ANOVA test). EPO was administered during dialysis before transplantation and was not measured in the circulation.

Recipient demographic (date of birth, date of transplantation, cause of ESRD, ethnicity, sex, and dialysis modality) and biologic data (serum iron, ferritin, transferrin, TSAT, TIBC, serum creatinine, cell blood count, and C-reactive protein) were collected on the day of transplantation and again on the seventh day after renal transplantation for serum creatinine levels. Characteristics of donors (living or brain-dead donor, donor age and sex, presence of reversible cardiac arrest, and dual kidney transplantation) and transplantation (combined transplants including kidney, delayed graft function, and acute graft rejection before discharge) were collected from the clinical charts of eligible patients.

eGFR on the seventh day after transplant was calculated with the eGFR_{MDRD}. mGFR was determined by renal clearance of ⁵¹Cr-EDTA 12 months after transplantation. Briefly, renal clearance of ⁵¹Cr-EDTA was determined after a single intravenous bolus injection of ⁵¹Cr-EDTA. After allowing 1 hour for distribution of the tracer in the extracellular fluid, renal ⁵¹Cr-EDTA clearance was determined on six consecutive 30-minute clearance periods. When timed urine samples could not be obtained or mean urine flow was below 1 ml/min, plasma clearance of ⁵¹Cr-EDTA was calculated using monoexponential analysis with the Brochner–Mortensen correction. mGFR was normalized to body surface area, which was calculated with the Mosteller formula.

Mice

All experiments were conducted using male mice. C57BL/6 (7–12 weeks old; 20–25 g) were from Charles River Laboratories. C57BL/6Ly5.1 congenic mice (B6.SJL-Ptprca Pep3b/BoyOrl) were from TAAM-CNRS Orleans USP44. *Hfe*^{-/-} mice (12–14 weeks old) are in a C57Bl6/129Sv mixed background. The WT (*Hfe*^{+/+}) mice are littermate controls. *Nrf2*^{-/-} mice generated by Masayuki Yamamoto (Tohoku University Graduate School of Medicine, Sendai, Japan) were obtained from RIKEN Bioresource Center.

Surgical Protocol

Animals were anesthetized by an intraperitoneal injection of ketamine: xylazine (100:10 mg/kg) solution. Animals (maintained at 37°C) were subjected to median incision, and both renal pedicles were crossclamped for 40 (C57BL/6 background) or 45 (129/sv background) minutes. This time difference was chosen due to differences in the sensitivity of the two genetic backgrounds to IRI. After the clamps were removed, the flank incision was closed with 4-0 silk sutures. The animals received warm saline instilled into the peritoneal cavity during the procedure. Mice were returned to cages for 24 hours. After 24 hours of reperfusion, animals were reanesthetized, blood was collected by retro-orbital bleeding, and kidneys were removed for analyses.

Generation of Chimeric Mice

The bone marrow from the tibia and femur of donor mice (12 weeks old; 23–25 g) was harvested. Bones were flushed under sterile conditions with RPMI-1640 (Invitrogen) containing 10% FCS. Cells were washed and resuspended in PBS containing 1% BSA, and viable cells were counted. Recipient WT and *Hfe*^{-/-} animals (12 weeks old) were sublethally irradiated (9 Gy). Reconstitution was performed 4 hours after irradiation with 5 × 10⁶ bone marrow cells. Chimeric mice were used 10 weeks after bone marrow transfer. The origin of donor or recipient cells was determined by congenic marker staining (Ly5.1

versus Ly5.2). In our conditions, reconstitution efficiency was nearly 98%. Four groups of chimeric mice were generated:

$$\text{WT}_{\text{Ly5.2}} \rightarrow \text{WT}_{\text{Ly5.1}}, \text{WT}_{\text{Ly5.1}} \rightarrow \text{WT}_{\text{Ly5.2}}, \\ \text{Hfe}^{-/-}_{\text{Ly5.2}} \rightarrow \text{WT}_{\text{Ly5.1}}, \text{ and } \text{WT}_{\text{Ly5.1}} \rightarrow \text{Hfe}^{-/-}_{\text{Ly5.2}}.$$

Peritonitis Model

Mice were injected daily (intraperitoneally) with 4.5 mg/kg Venofer (iron sucrose solution) or vehicle (*i.e.*, sodium hydroxide at pH 10.5–11) for 10 days. Peritonitis was induced by intraperitoneal injection of LPS (7.5 mg/kg) 2 hours after the last treatment. Animals were euthanized 12 hours later. Mice received 10 ml PBS containing 0.5% BSA and 2 mM EDTA into the peritoneal cavity. After injection, cells were dislodged by gentle massage of the abdomen. Peritoneal fluids were collected using a 21-gauge needle attached to a 10-ml syringe, and cells were washed.

In Vivo Depletion of Monocytes/Macrophages and Adoptive Transfer

Clodronate liposomes were purchased from Nico van Rooijen (Vrije University, Amsterdam, The Netherlands; <http://www.clodronateliposomes.org>). After warming and resuspension of liposomes, a dose of 200 μl was administered intravenously by retro-orbital injection to induce monocyte/macrophage depletion. The control group was injected with liposomes containing PBS. BMMs (5 × 10⁶ cells per animal) were administered intravenously by retro-orbital injection at 1 hour after reperfusion.

Serum Iron and Kidney Function Parameters

Mouse serum iron, transferrin, ferritin, urea, and creatinine levels were measured using the AU400 chemistry analyzer (Olympus). TSAT was calculated by dividing serum iron concentration by TIBC.

Histology and Immunohistochemistry

Paraffin-embedded kidney sections (4 μm in thickness) were stained by Masson trichrome. Morphologic blind assessment was performed by an experienced renal pathologist (M.F.). Tubular necrosis score was established for each animal by assessing the intensity of tubular lesions (null, mild, or important) in ten randomly chosen fields in the corticomedullary junction. Global tubular injury scores were expressed in percentages.

For immunohistochemistry, frozen kidney sections were incubated with anti-mouse CD11b biotinylated antibody (clone M1/70; BD Biosciences) for 1 hour at room temperature and anti-mouse F4/80 (clone Cl:A3-1; Bio-Rad, Hercules, CA) or anti-mouse GR1 antibody (clone RB6-8C5; BD Biosciences) overnight at 4°C followed by incubation with biotinylated anti-rat IgG (SouthernBiotech) for 1 hour at room temperature. These were followed by incubation with streptavidin-HRP for 30 minutes (Vectastain; ABC kit; Vector Laboratories), which was revealed by immunoperoxidase reaction (Dako; Carpinteria). Slides were mounted with the Eukitt mounting medium (Electron Microscopy Sciences) and observed under an upright microscope (DM2000; Leica) using the IM50 software (Leica).

Culture of BMMs

BMMs were grown from myeloid precursors obtained from the femurs and tibias of 6- to 8-week-old C57BL/6 mice. Bone marrow cells

were cultured for 7 or 8 days at 37°C at 2×10^6 cells per 1 ml in RPMI-1640 medium (Invitrogen) containing 10% FCS (Biowest), penicillin/streptomycin, and 15% (vol/vol) supernatant of L929 cells as a source of M-CSF in the presence or absence of FeCl_3 -nitrilotriacetate (FeCl_3 -NTA; 10–60 μM as indicated). In some conditions, LPS (150 ng/ml; Sigma-Aldrich), peptidoglycan (15 $\mu\text{g}/\text{ml}$), and Poly-IC (50 $\mu\text{g}/\text{ml}$; Cayla-Invivogen, Toulouse, France) were added 12 hours before BMM analysis on day 8.

Leukocyte Counts

Blood samples from mice were collected in EDTA-coated tubes and analyzed for leukocyte count in an MS9–5 Blood Analyzer (Melet Schloesing Laboratories) according to the manufacturer's instructions.

Flow Cytometry

Cells from cell cultures or mouse tissues were suspended in PBS and incubated with anti-Fc γ R mAb 2.4G2 to block IgG receptors before cell staining for specific surface markers. Cells (1×10^6) were then stained at 4°C in PBS containing 1% BSA with antibodies against mouse CD11b (M1/70; BioLegend), F4/80 (BM8; eBioscience), CD86 (GL-1; BioLegend), Ly6G (1A8; BD Biosciences), and Ly6C (HK1.4; BioLegend). Macrophages were CD11b⁺ F4/80⁺ Ly6G[−] cells.

For NRF2 analysis, BMMs were differentiated in the absence or presence of iron (FeCl_3 -NTA at 10, 20, or 60 μM). On culture day 7, cells (1×10^6) were washed, permeabilized with the Foxp3 Fixation/Permeabilization Concentrate and Diluent Kit (eBioscience), and stained with anti-NRF2 purified antibody at 4°C for 30 minutes. Macrophages were then incubated with secondary Alexa488-conjugated anti-rabbit IgG at 4°C and stained for 5 minutes with 1 μM Draq5 (as a nuclear stain) at room temperature before analysis. Image acquisition was performed with the ImageStream multispectral imaging flow cytometer, and acquired images were analyzed with the IDEAS software. Cytoplasmic to nuclear translocation of NRF2 transcription factor was measured using the similarity score, which simply quantifies the intensity values of the nuclear and cytoplasmic NRF2 protein image pixels.

Cytokine Production

Kidney tissues were homogenized in 300 μl RIPA buffer supplemented with phosphatase and protease inhibitor cocktail (Sigma-Aldrich) for 30 seconds. Samples were cooled on ice for 30 minutes. Lysates were centrifuged at $10,000 \times g$ at 4°C. IL-6, TNF- α , MCP-1, IL-10, and IL-12 were measured simultaneously by cytometric bead array using the mouse inflammation kit according to the manufacturer's instructions (BD Biosciences). Results were analyzed using FCAP array software. Proteins were quantified in supernatants by the bicinchoninic acid method according to the manufacturer's instructions (Pierce). Cytokine concentrations were normalized to total protein and expressed as picograms per milligram total tissue proteins.

GeneChip Microarrays

To examine gene expression, total RNA (100 ng) extracted from BMM stimulated or not with LPS was quality controlled, processed following Affymetrix recommendations, and hybridized to the mouse GeneChip array (Affymetrix 430 v2.0). Signals were normalized for each array, and samples were compared.

Quantitative Real-Time RT-PCR

Total RNA was extracted from BMMs (RNeasyPlus Mini Kit; Qiagen) and quantified with a Nanodrop system. RNA quality was assessed by OD reading at the 260-to-280-nm ratio and by agarose gel electrophoresis. Reverse transcription was carried out from 500 ng total RNA using the iScript reverse transcription Supermix (Bio-Rad). Real-time PCR was performed using SsoFast EvaGreen Supermix (Bio-Rad). The following sequences of primers obtained from Eurofins MWG Operon (Ebersberg, Germany) were used: IL-6: (forward) 5'-CCACGGCCTTCCCTACTTCA-3', (reverse) 5'-GCCATTGCA-CAACTCTTTTCTCAT-3'; TNF- α : (forward) 5'-GTAGCC-CACGTCGTAGCAAACCACC-3', (reverse) 5'-TGGGGCAGGGGCTCTT-GACG-3'; β -actin: (forward) 5'-GGCTGTATTCCCCTCCATCG-3', (reverse) 5'-CCAGTTGGTAAACAATGCCATGT-3'; and GAPDH: (forward) 5'-ACGGCAAATTCAACGGCACAGTCA-3', (reverse) 5'-TGGGGGCATCGGCAGAAGG-3'. Gene quantification was performed in duplicate using the CFX96 PCR System (Bio-Rad). Data were normalized to GAPDH and β -actin values in a combined way.

ROS Assessment

BMMs were stimulated by LPS (150 ng/ml) to induce ROS production. After 3 hours, BMMs were washed with PBS, and 5 μM dichlorodihydrofluorescein-diacetate was added and incubated for 20 minutes at 37°C. Cells were washed again and taken to the flow cytometer for ROS analysis. FeCl_3 -NTA was used as mentioned before, and NaOH was used as the vehicle.

Statistical Analyses

For human studies, Fisher exact or chi-squared tests were used to analyze categorical data. Mann–Whitney or unpaired *t* tests were used to analyze continuous numerical data, Pearson tests were used to study correlation between eGFR_{MDRD} and ferritin levels, and multiple regression analysis was used to compare determinants of kidney allograft outcome according to maximum likelihood criteria. An arbitrary cutoff value of 45 ml/min per 1.73 m², corresponding to the threshold value below which stage 3b of chronic renal disease is defined according to KDIGO 2013, was used to define either good or bad kidney graft function outcome. Moreover, this value is close to the median value of GFR in the transplanted population, leading to an equal distribution of patients on both sides of this threshold. Survival was studied through plotting of Kaplan–Meier curves and log rank test. All analyses were performed with SAS9.1 software (SAS Institute, Cary, NC).

For experimental studies, statistical analyses were performed with GraphPad Prism (version 5.0; GraphPad Software); *t* tests were used for all comparisons. A *P* value <0.05 was considered significant.

ACKNOWLEDGMENTS

We thank Dr. Andrews (Duke University School of Medicine) and Prof. Yamamoto (Tohoku University Graduate School of Medicine, Sendai, Japan) for *Hfe*^{−/−} and *Nrf2*^{−/−} mice, respectively. We acknowledge the skillful technical assistance of S. Nelson, J. Bex, and O. Thibaudau.

This work was supported by Agence Nationale de la Recherche (ANR) grants ANR-10-JCJC-1108, ANR-12-BSV1-0039, and ANR-11-LABX-0051; de l'Assistance Publique-Hôpitaux de Paris et du Centre National de la Recherche Scientifique Contrat Hospitalier de Recherche Translationnelle; the Fondation pour la Recherche Médicale; the Association Laurette Fugain, and Association pour la Recherche sur le Cancer. C.V. was supported by grants from the Société Française d'Hématologie and Ministère de l'Enseignement Supérieur et de la Recherche.

DISCLOSURES

None.

REFERENCES

- Hariharan S, Johnson CP, Bresnahan BA, Taranto SE, McIntosh MJ, Stablein D: Improved graft survival after renal transplantation in the United States, 1988 to 1996. *N Engl J Med* 342: 605–612, 2000
- Tilney NL, Guttman RD: Effects of initial ischemia/reperfusion injury on the transplanted kidney. *Transplantation* 64: 945–947, 1997
- Herrero-Fresneda I, Torras J, Cruzado JM, Condom E, Vidal A, Riera M, Lloberas N, Alsina J, Grinyo JM: Do alloreactivity and prolonged cold ischemia cause different elementary lesions in chronic allograft nephropathy? *Am J Pathol* 162: 127–137, 2003
- Alejandro V, Scandling JD Jr., Sibley RK, Dafoe D, Alfrey E, Deen W, Myers BD: Mechanisms of filtration failure during postischemic injury of the human kidney. A study of the reperfused renal allograft. *J Clin Invest* 95: 820–831, 1995
- Perico N, Cattaneo D, Sayegh MH, Remuzzi G: Delayed graft function in kidney transplantation. *Lancet* 364: 1814–1827, 2004
- Sonnweber T, Theurl I, Seifert M, Schroll A, Eder S, Mayer G, Weiss G: Impact of iron treatment on immune effector function and cellular iron status of circulating monocytes in dialysis patients. *Nephrol Dial Transplant* 26: 977–987, 2011
- Oexle H, Kaser A, Möst J, Bellmann-Weiler R, Werner ER, Werner-Felmayer G, Weiss G: Pathways for the regulation of interferon-gamma-inducible genes by iron in human monocytic cells. *J Leukoc Biol* 74: 287–294, 2003
- Weiss G: Iron and immunity: A double-edged sword. *Eur J Clin Invest* 32[Suppl 1]: 70–78, 2002
- Wang L, Harrington L, Trebicka E, Shi HN, Kagan JC, Hong CC, Lin HY, Babitt JL, Cherayil BJ: Selective modulation of TLR4-activated inflammatory responses by altered iron homeostasis in mice. *J Clin Invest* 119: 3322–3328, 2009
- Pagani A, Nai A, Corna G, Bosurgi L, Rovere-Querini P, Camaschella C, Silvestri L: Low hepcidin accounts for the proinflammatory status associated with iron deficiency. *Blood* 118: 736–746, 2011
- Franks I: Transplantation: Expression levels of iron homeostasis genes predict liver graft tolerance. *Nat Rev Gastroenterol Hepatol* 9: 62, 2012
- Bhattacharyya S, Ghosh J, Sil PC: Iron induces hepatocytes death via MAPK activation and mitochondria-dependent apoptotic pathway: Beneficial role of glycine. *Free Radic Res* 46: 1296–1307, 2012
- Deb S, Johnson EE, Robalinho-Teixeira RL, Wessling-Resnick M: Modulation of intracellular iron levels by oxidative stress implicates a novel role for iron in signal transduction. *Biometals* 22: 855–862, 2009
- Muñoz P, Zavala G, Castillo K, Aguirre P, Hidalgo C, Núñez MT: Effect of iron on the activation of the MAPK/ERK pathway in PC12 neuroblastoma cells. *Biol Res* 39: 189–190, 2006
- Yuan X, Cong Y, Hao J, Shan Y, Zhao Z, Wang S, Chen J: Regulation of LIP level and ROS formation through interaction of H-ferritin with G-CSF receptor. *J Mol Biol* 339: 131–144, 2004
- Pham CG, Bubici C, Zazzeroni F, Papa S, Jones J, Alvarez K, Jayawardena S, De Smaele E, Cong R, Beaumont C, Torti FM, Torti SV, Franzoso G: Ferritin heavy chain upregulation by NF-kappaB inhibits TNFalpha-induced apoptosis by suppressing reactive oxygen species. *Cell* 119: 529–542, 2004
- Drüeke TB, Parfrey PS: Summary of the KDIGO guideline on anemia and comment: Reading between the (guide)line(s). *Kidney Int* 82: 952–960, 2012
- Eckardt KU, Kasiske BL: Kidney disease: Improving global outcomes. *Nat Rev Nephrol* 5: 650–657, 2009
- Bonventre JV, Yang L: Cellular pathophysiology of ischemic acute kidney injury. *J Clin Invest* 121: 4210–4221, 2011
- Ajioka RS, Levy JE, Andrews NC, Kushner JP: Regulation of iron absorption in Hfe mutant mice. *Blood* 100: 1465–1469, 2002
- Chen GY, Nuñez G: Sterile inflammation: Sensing and reacting to damage. *Nat Rev Immunol* 10: 826–837, 2010
- Feder JN, Gnirke A, Thomas W, Tsuchihashi Z, Ruddy DA, Basava A, Dormishian F, Domingo R Jr., Ellis MC, Fullan A, Hinton LM, Jones NL, Kimmel BE, Kronmal GS, Lauer P, Lee VK, Loeb DB, Mapa FA, McClelland E, Meyer NC, Mintier GA, Moeller N, Moore T, Morikang E, Prass CE, Quintana L, Stames SM, Schatzman RC, Brunke KJ, Drayna DT, Risch NJ, Bacon BR, Wolff RK: A novel MHC class I-like gene is mutated in patients with hereditary haemochromatosis. *Nat Genet* 13: 399–408, 1996
- Ghosh EE, Cassado AA, Govoni GR, Fukuhara T, Yang Y, Monack DM, Bortoluci KR, Almeida SR, Herzenberg LA, Herzenberg LA: Two physically, functionally, and developmentally distinct peritoneal macrophage subsets. *Proc Natl Acad Sci U S A* 107: 2568–2573, 2010
- Mosser DM, Edwards JP: Exploring the full spectrum of macrophage activation. *Nat Rev Immunol* 8: 958–969, 2008
- Ma Q: Role of nrf2 in oxidative stress and toxicity. *Annu Rev Pharmacol Toxicol* 53: 401–426, 2013
- Niture SK, Khatri R, Jaiswal AK: Regulation of Nrf2—an update. *Free Radic Biol Med* 66: 36–44, 2014
- Ruiz S, Pergola PE, Zager RA, Vaziri ND: Targeting the transcription factor Nrf2 to ameliorate oxidative stress and inflammation in chronic kidney disease. *Kidney Int* 83: 1029–1041, 2013
- Kobayashi A, Kang MI, Okawa H, Ohtsuji M, Zenke Y, Chiba T, Igarashi K, Yamamoto M: Oxidative stress sensor Keap1 functions as an adaptor for Cul3-based E3 ligase to regulate proteasomal degradation of Nrf2. *Mol Cell Biol* 24: 7130–7139, 2004
- Itoh K, Chiba T, Takahashi S, Ishii T, Igarashi K, Katoh Y, Oyake T, Hayashi N, Satoh K, Hatayama I, Yamamoto M, Nabeshima Y: An Nrf2/small Maf heterodimer mediates the induction of phase II detoxifying enzyme genes through antioxidant response elements. *Biochem Biophys Res Commun* 236: 313–322, 1997
- Eisenga MF, Minović I, Berger SP, Kootstra-Ros JE, van den Berg E, Riphagen IJ, Navis G, van der Meer P, Bakker SJ, Gaillard CA: Iron deficiency, anemia, and mortality in renal transplant recipients. *Transpl Int* 29: 1176–1183, 2016
- Callens C, Coulon S, Naudin J, Radford-Weiss I, Boissel N, Raffoux E, Wang PH, Agarwal S, Tamouza H, Paubelle E, Asnafi V, Ribeil JA, Dessen P, Canioni D, Chandesaris O, Rubio MT, Beaumont C, Benhamou M, Dombret H, Macintyre E, Monteiro RC, Moura IC, Hermine O: Targeting iron homeostasis induces cellular differentiation and synergizes with differentiating agents in acute myeloid leukemia. *J Exp Med* 207: 731–750, 2010
- Henique C, Bollee G, Lenoir O, Dhaun N, Camus M, Chipont A, Flosseau K, Mandet C, Yamamoto M, Karras A, Thervet E, Bruneval P, Nochy D, Mesnard L, Tharaux PL: Nuclear factor erythroid 2-related factor 2 drives podocyte-specific expression of peroxisome proliferator-activated receptor γ essential for resistance to crescentic GN. *J Am Soc Nephrol* 27: 172–188, 2016

This article contains supplemental material online at <http://jasn.asnjournals.org/lookup/suppl/doi:10.1681/ASN.2016080926/-/DCSupplemental>.